PHYSICAL REVIEW B VOLUME 36, NUMBER 7 1 SEPTEMBER 1987

Local spin and orbital moment in $Nd_2Fe_{14}B$ and Y_2Fe_{17}

Barbara Szpunar* and W. E. Wallace
Mellon Institute, Carnegie Mellon University, Pittsburgh, Pennsylvania 15213

Jerzy Szpunar
Department of Mining and Metallurgical Engineering, McGill University, Montreal, Canada H3A 2A7

(Received 23 June 1986; revised manuscript received 10 November 1986)

The local spin and orbital moments have been calculated on the six different sites of iron atoms in $Nd_2Fe_{14}B$ and on four different sites of iron in Y_2Fe_{17}. The continued-fraction technique has been used in these calculations. The calculated values are discussed in the light of experimental data.

I. INTRODUCTION

It has been thought until recently that to obtain high-performance permanent magnets the presence of cobalt is essential. $SmCo_5$ has been widely used in applications. However, for large-scale adaptation it is necessary to eliminate cobalt as it is a costly material and is of limited availability.

It has been suggested in our previous calculations[1] that the $CaCu_5$ structure is essential to obtain high anisotropy on transition-metal sites. Such a structure, however, does not exist in rare-earth–Fe intermetallic compounds. It has been found recently that by adding boron one can obtain in these compounds a tetragonal structure (Fig. 1) which is related to the hexagonal $CaCu_5$ structure.[2,3]

Local-symmetry analysis for $Nd_2Fe_{14}B$ has been done recently by Herbst *et al.*[2,4] Their analysis demonstrated the importance of the contribution of the iron sites to the uniaxial anisotropy.[4,5] The anisotropy of the rare-earth sites is also important, i.e., H_A for $Y_2Fe_{14}B$ is 27.3 kOe and 70.7 kOe for $Nd_2Fe_{14}B$. The iron contribution to uniaxial anisotropy in $Nd_2Fe_{14}B$ is most significant at higher temperatures where high uniaxial anisotropy is observed. It is known that the direct interaction of transition-metal atoms is stronger and less temperature dependent than the indirect interaction which exists between rare-earth atoms,[6] and at low temperatures the observed cone structure in $Nd_2Fe_{14}B$ is probably due to the effect of the neodymium crystal field. Understanding the origin of the high magnetic moment is also a goal of our calculations. So far only the total of the magnetic moment has been measured and the agreement between the values obtained using different methods is poor.[4,7–10] However, all the experimental data suggests that the site with the highest magnetic moment is the 8_{j2} site.

II. THEORETICAL MODEL

The complexity of the $Nd_2Fe_{14}B$ structure is such that simplifying approximations have to be made in order to carry out band-structure calculations.

We assume that Hubbard's tight-binding Hamiltonian, in the Hartree-Fock approximation, describes the magnetic properties of d electrons in rare-earth transition-metal compounds well.[11,12] This Hamiltonian can be formulated as

$$H=\sum_{i,s}\varepsilon_{is}c_{is}^{\dagger}c_{is}+\sum_{i\,(\neq j),s}t_{ij}c_{is}^{\dagger}c_{js}\ , \qquad (1)$$

where $c_{is}^{\dagger},c_{is}$ are, respectively, the creation and annihilation operators on site i, and s is the spin quantum number. The energy ε_{is} for iron atoms is

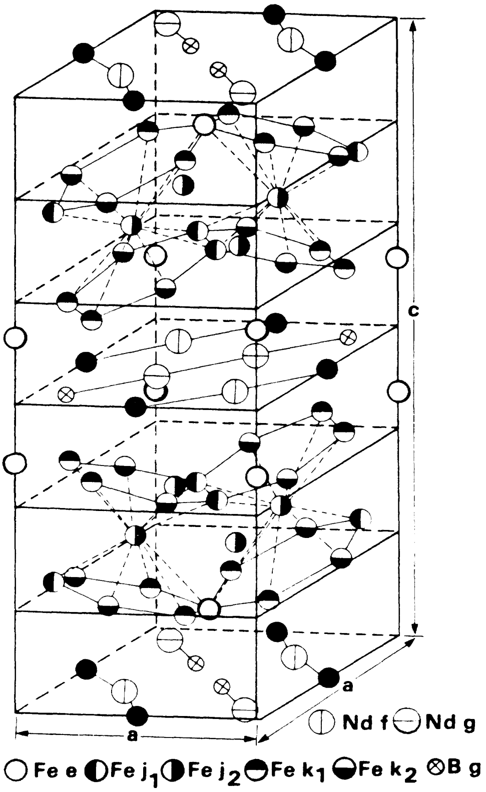

FIG. 1. Unit cell of $Nd_2Fe_{14}B$ ($P4_2/mnm$ space group) after Herbst *et al.* (Ref. 2).

$$\varepsilon_{is}=\varepsilon_{\mathrm{Fe}}+U_{\mathrm{Fe}}\langle n_{i-s}\rangle , \tag{2}$$

and for neodymium atoms (in the mean-field approximation[6,11]

$$\begin{aligned}\varepsilon_{is}=\varepsilon_{\mathrm{Nd}}&+U_{\mathrm{Nd}}\langle n_{i-s}\rangle\\ &-I\,|(\lambda-1)j\,|\,\mathrm{sgn}[(\langle n_{is}\rangle-\langle n_{i-s}\rangle)I] ,\end{aligned} \tag{3}$$

where $\varepsilon_{\mathrm{Fe}}$ and $\varepsilon_{\mathrm{Nd}}$ are, respectively, the atomic energy levels of Fe and Nd. In the above U_{Fe} and U_{Nd} are the intra-atomic Coulomb-repulsion constants, $\langle n_{\mathrm{is}}\rangle$ the average number of electrons on site i with spin quantum number s, λ is the Landé factor, j is the total-moment quantum number, and t_{ij} in formula (1) is the transfer term between nearest neighbors. The combination of the difference between the values of the atomic energy levels of the transition-metal and rare-earth (R) metal ($\varepsilon_{\mathrm{Fe}},\varepsilon_R$) and the large band splitting on the transition-metal site causes antiferromagnetic coupling between the spins of the conduction electrons of the transition and rare-earth metals.[13] The last term in expression (3) represents the exchange interaction of the band electrons (d) with the localized spin of f electrons. In a previous paper[14] we assumed that the exchange interaction between localized spin and conduction electrons for rare-earth metals is positive, and almost a universal constant ($I=0.05$ eV).[14] Since the Landé factor (λ) for Nd is less than 1 ($\frac{8}{11}$), the localized spin on the neodymium site is antiparallel to the total moment [$S=(\lambda-1)j$]. However, the spin moments of conduction electrons of neodymium and iron couple in an antiparallel fashion. Thus we observe ferromagnetic coupling between the total local moment of the Nd site and the iron site.[3,4,15] The coupling between d electrons of rare-earth and transition metals is a result of a direct interaction and, unlike superexchange interactions, does not change much with the distance between atoms.

The continued-fraction technique is used for calculating the density of states. In this method the Hamiltonian is a tridiagonal matrix, by use of a special orthonormal set of basis functions. This leads to an expression for the local electronic density of states which has the form of a continued fraction. The Green's function, whose imaginary part describes the density of states, is a continued fraction and has the following form:

$$\langle 0\,|\,G(\varepsilon)\,|\,0\rangle G_{00}(\varepsilon)=\cfrac{b_0^2}{\varepsilon-a_0-\cfrac{b_1^2}{\varepsilon-a_1-\cfrac{b_2^2}{\varepsilon-a_2-\ddots\; t(\varepsilon)}}} , \tag{4}$$

where $t(\varepsilon)$ is a terminator of the continued fraction. In the presence of a significant diagonal disorder the continued fraction coefficients may not be convergent, and certain features of the density of states may depend on the terminator of the continued fraction. It has been shown, however, that the integrated values of various quantities such as the magnetic moment do not depend on the terminator if weights in the band are protected.[16] In this work we use the terminator proposed by Beer and Pettifor[17] as it protects the weights in the band and is useful in the estimation of the integrated quantities. We neglect s and p electrons in our calculations. We believe we can do this since it is mainly the d electrons which contribute to the magnetic moment of the transition metals. Due to hybridization, the s and p electrons might affect the shape of the density of states of the d electrons. The influence of s and p electrons on integrated values, such as magnetic moments, are not significant. In our previous calculations[18] on $Nd_2Fe_{14}B$, we found that boron atoms expand Fe-Fe interatomic distances and therefore stabilize the tetragonal symmetry. We have also demonstrated that we can neglect the contribution of the electrons of boron atoms to the local magnetic moment.

III. THE CALCULATIONS OF THE LOCAL-SPIN MOMENT AND LOCAL-ORBITAL MOMENT

At zero temperature the spin-flip scattering can be neglected, and we can calculate the paramagnetic density of states, taking into account the shifting (ΔE) of the center of the density of states for spin-up electrons towards the density of states for the spin-down electrons. The band splitting can be calculated using the Stoner method:

$$\Delta E=\tilde{U}m , \tag{5}$$

where $\tilde{U}$ is an effective intra-atomic Coulomb energy and m is the magnetic moment of the d electrons. Then we can calculate self-consistently, from five-fold-degenerate band electrons, the contribution of the local spin (S_i) using the formula

$$S_i=\tfrac{1}{2}g_s\mu_B\sum_{\nu=1}^{5}(\langle n_{i\uparrow}^{\nu}\rangle-\langle n_{i\downarrow}^{\nu}\rangle) , \tag{6}$$

where g_s is the gyromagnetic factor, μ_B is the Bohr magneton, and

$$\langle n_{is}^{\nu}\rangle=\int_{-\infty}^{\varepsilon_F}\rho_{is}^{\nu}(\omega)d\omega . \tag{7}$$

TABLE I. Real angular wave functions for d electrons ($l=2$).

$\|m\|$	$\psi_{l\|m\|}$
2	$\sqrt{15}/2\frac{x^2-y^2}{r^2}$, $\sqrt{15}\frac{xy}{r^2}$
1	$\sqrt{15}\frac{xz}{r^2}$, $\sqrt{15}\frac{y^2}{r^2}$
0	$\sqrt{5/2}\frac{3z^2-r^2}{r^2}$

The upper limit in this integral is the Fermi energy ε_F, and $\rho_{is}^{v}(\omega)$ is a partial density of states on site i corresponding to the real wave functions for d electrons with $|m|=v$ (see Table I)—it is calculated separately for spin-up and -down electrons.

The spin-orbit interaction also affects the splitting of the partial density of states. The form of the spin-orbit interaction can be calculated from Dirac's relativistic wave equation for low-energy electrons, and in a central field potential the spin-orbit interaction has the form

$$\Delta(s\text{-}o)=\xi\hat{l}\cdot\hat{s} \ , \tag{8}$$

where $\hat{l}$ and $\hat{s}$ are the orbital- and spin-angular-momentum operators.

When $s=\frac{1}{2}$ the spin-orbit energy can be written as

$$\Delta(s\text{-}o)^{(j=l+1/2)}=l(\xi/2)=lE(s\text{-}o) \tag{9}$$

and

$$\Delta(s\text{-}o)^{(j=l-1/2)}=-(l+1)(\xi/2)=-(l+1)E(s\text{-}o) \ , \tag{10}$$

where l is the orbital-angular-momentum quantum number and j is the total-angular-momentum quantum number.[19]

For $s=\frac{1}{2}$ we can calculate the proportion of electrons having a given j and also calculate the projections of the orbital angular momentum (m).[20] The results are presented in Table II. The proportion of electrons with various j,m can also be calculated directly from Clebsch-Gordan coefficients using the definition (4) above, treating spin-up and -down electrons separately. Having calculated the density of states using the recursion method for different wave functions of d electrons (Table I), we obtain the decomposed density of states by splitting the corresponding components according to formulas (9) and (10).[19]

The oribtal moment can then be calculated using the formula

$$m_l=g_l\mu_B\sum_{m=-2}^{2}m\int_{-\infty}^{\varepsilon_F}\rho_l^m(\omega)d\omega \ , \tag{11}$$

where $\rho_l^m(\omega)$ is a decomposed partial density of states of d electrons with an azimuthal quantum number m.

IV. RESULTS AND DISCUSSION

The method of calculation presented above requires knowledge of a few parameters, such as the transfer terms (t_{ij}), which in a tight-binding scheme are related to the Slater-Koster[21,22] two-center hopping integrals, atomic energy levels ε_i, the Coulomb exchange interaction (U_i), and the spin-orbit interaction constant $E(s\text{-}o)$. The tight-binding parameters have been calculated using the Pettifor formula.[21] For d electrons of various symmetries they are

$$dd\chi=\left\{\begin{array}{c}-60.0\\+40.0\\-10.0\end{array}\right\}\times\frac{W_d}{25}(S/R)^5 \ \text{ for } \chi=\left\{\begin{array}{c}\sigma\\\pi\\\delta\end{array}\right. \tag{12}$$

where S is the Wigner-Seitz radius, W_d is the width of the d band, and R is the distance to the nearest neighbor. The hopping parameters between different types of atoms (i,j) have been calculated using the Shiba approximation:[23]

$$dd\chi_{ij}=\sqrt{dd\chi_i dd\chi_j} \ . \tag{13}$$

Unlike the local moments of transition metals, the induced magnetic moments on rare-earth–metal sites depend on the values of the atomic energy levels (ε_{is}). The parameter ε_{is} is determined self-consistently so that it depends only on the type of atom occupying the ith site; therefore, we have chosen the same values for $\varepsilon_{\uparrow}^{\mathrm{Fe}}$ and $\varepsilon_{\downarrow}^{\mathrm{Fe}}$ in $Nd_2Fe_{14}B$ and in Y_2Fe_{17}. The atomic energy level of iron, for spin-up and -down electrons, was set equal to $\varepsilon_{\uparrow}^{\mathrm{Fe}}=-0.18$ Ry and $\varepsilon_{\downarrow}^{\mathrm{Fe}}=-0.08$ Ry, respectively. For spin-down and -up electrons of yttrium and neodymium, we have $\varepsilon_{\uparrow\downarrow}^{R}=0.0$ Ry. This corresponds to an effective Coulomb exchange interaction ($\tilde{U}=U/5$) of 0.045 Ry, giving an average moment of $2.2\mu_B$ per Fe atom in Y_2Fe_{17}. The $\tilde{U}$ value used in our calculation is comparable to the value of U (2.4 eV) for pure iron used by Cox *et al.*[24] We can separate the local moment on neodymi-

TABLE II. Proportion of d electrons corresponding to spin up and down for different m values ($j=l\pm\frac{1}{2}$) (Ref. 20).

	Spin up		Spin down	
m	$j=2.5$	$j=1.5$	$j=2.5$	$j=1.5$
-2	$\frac{1}{10}$	$\frac{4}{10}$	$\frac{1}{2}$	0
2	$\frac{1}{2}$	0	$\frac{1}{10}$	$\frac{4}{10}$
-1	$\frac{2}{10}$	$\frac{3}{10}$	$\frac{4}{10}$	$\frac{1}{10}$
1	$\frac{4}{10}$	$\frac{1}{10}$	$\frac{2}{10}$	$\frac{3}{10}$
0	$\frac{3}{5}$	$\frac{2}{5}$	$\frac{2}{5}$	$\frac{3}{5}$

TABLE III. Calculated and measured magnetic- (m), spin- (m_s), and orbital-moment (m_l) contributions of band electrons for different sites of iron in $Nd_2Fe_{14}B$.

Presented values	Fe (4c)	Fe (4e)	Occupation number and site Fe ($8j_1$)	Fe ($8j_2$)	Fe ($16k_1$)	Fe ($16k_2$)
m_s^{th} (units of μ_B)	2.49	2.42	2.33	2.61	2.40	2.40
m_l^{th} (units of μ_B) $E(s\text{-}o)=0.0027$ Ry	0.02	0.02	0.00	0.11	0.05	0.03
m_l^{th} (units of μ_B) $E(s\text{-}o)=0.004$ Ry	0.03	0.05	0.00	0.16	0.08	0.04
m^{th} $E(s\text{-}o)=0.0027$ Ry	2.51	2.44	2.33	2.72	2.45	2.43
m^{exp} (77 K)[a]	2.2	1.1	2.7	3.5	2.4	2.4
m^{exp} (4.2 K)[b]	2.75	2.10	2.30	2.85	2.60	2.60
m^{exp} (80 K)[c]	2.52	2.41	2.07	2.37	2.20	2.37
m^{exp} ($c^{\text{d}}=\frac{1}{145}$ kG/μ_B)[e]	2.41	2.19	2.05	2.59	2.28	2.32
m^{exp} ($c^{\text{d}}=\frac{1}{145}$ kG/μ_B)[f]	1.83	1.74	1.99	2.37	1.97	2.12

[a] Reference 4.

[b] Reference 7.

[c] Reference 8.

[d] c=const used to calculate local moments from Mössbauer measurements of hyperfine fields.

[e] Reference 9.

[f] Reference 10.

um into two parts, one from localized $4f$ electrons and one from conduction electrons. The contribution of $4f$ electrons to the local moment on neodymium is $3.27\mu_B$. To calculate the total local moment we have to add to this value a small negative contribution due to the polarization of conduction electrons. We found the total local moment on the $4f$ site of neodymium to be $2.8\mu_B$ and $2.77\mu_B$ on the $4g$ site of neodymium.

There is some uncertainty about the value of $E(s\text{-}o)$ for iron atoms in the compound. The $E(s\text{-}o)$ constant calculated by Herman and Skillman[19] is 0.0027 Ry. As suggested in our previous paper,[25] we have performed calculations for higher values of $E(s\text{-}o)$, namely $E(s\text{-}o)=0.004$ Ry. The calculated spin contribution and the orbital moments for different sites of iron in $Nd_2Fe_{14}B$ and Y_2Fe_{17} are presented in Tables III and IV. The agreement between local moments measured by neutron-diffraction techniques[4,7] and Mössbauer spectroscopy[8,9,10] and the calculated values is satisfactory. This supports our approximation that mainly the strongly localized d electrons contribute to the magnetic moment.[11] The highest spin and orbital moment calculated for Fe was on the $8j_2$ site; this is in agreement with experiment.[4,7–10,26] There is no direct relation between the magnitude of the local moment and anisotropy; however, some correlation has been found in transition metals.[20] In our previous work[27] we found correlation between calculated local-orbital moments and local anisotropy on cobalt atoms in Y_2Co_{17}. We conclude that the $8j_2$ site, which makes the largest contribution to the orbital moment, is mainly responsible for the high uniaxial anisotropy in $Nd_2Fe_{14}B$. This is in agreement with recent Mössbauer measurements[26] and predictions.[28] The site corresponding to $8j_2$ for Y_2Fe_{17} is Fe(IV) ($4f$), which is where the highest magnetic moment has been calculated. The average moment on the iron sites in Y_2Fe_{17} is lower than on the iron sites in $Nd_2Fe_{14}B$. The calculated orbital moment has quite a large error, as it is calculated from the small splitting that is the difference between two large numbers. In our calculations we found the highest orbital moment on the $8j_2$ and four Fe(IV) sites. This might suggest that the main contribution to uniaxial anisotropy is coming from these two sites. This is reasonable when we look at the local symmetry. The local symmetry on $8j_2$ atoms is uniaxial as $8j_2$ atoms have been pulled out from the center of the hexagon (Fig. 1).[4] That the highest orbital moment is on four Fe(IV) sites is in agreement with the anisotropy measurements for $Gd_2(Co_{1-x}Fe_x)_{17}$.[29] The iron atoms prefer substitution in four Fe(IV) sites and the anisotropy changes from easy basal plane to uniaxial with increasing concentra-

TABLE IV. Calculated magnetic- (m), spin- (m_s), and orbital-moment (m_l) contributions of band electrons for different sites of iron in Y_2Fe_{17}.

Occupation number and site	Fe(II) (12j)	Fe(IV) (4f)	Fe(I) (6g)	Fe(III) (12k)
m_s (units of μ_B)	2.09	2.45	2.15	2.10
m_l (units of μ_B) $E(s\text{-}o)=0.0027$ Ry	0.05	0.09	0.00	−0.01
m_l (units of μ_B) $E(s\text{-}o)=0.004$ Ry	0.07	0.14	−0.02	−0.02

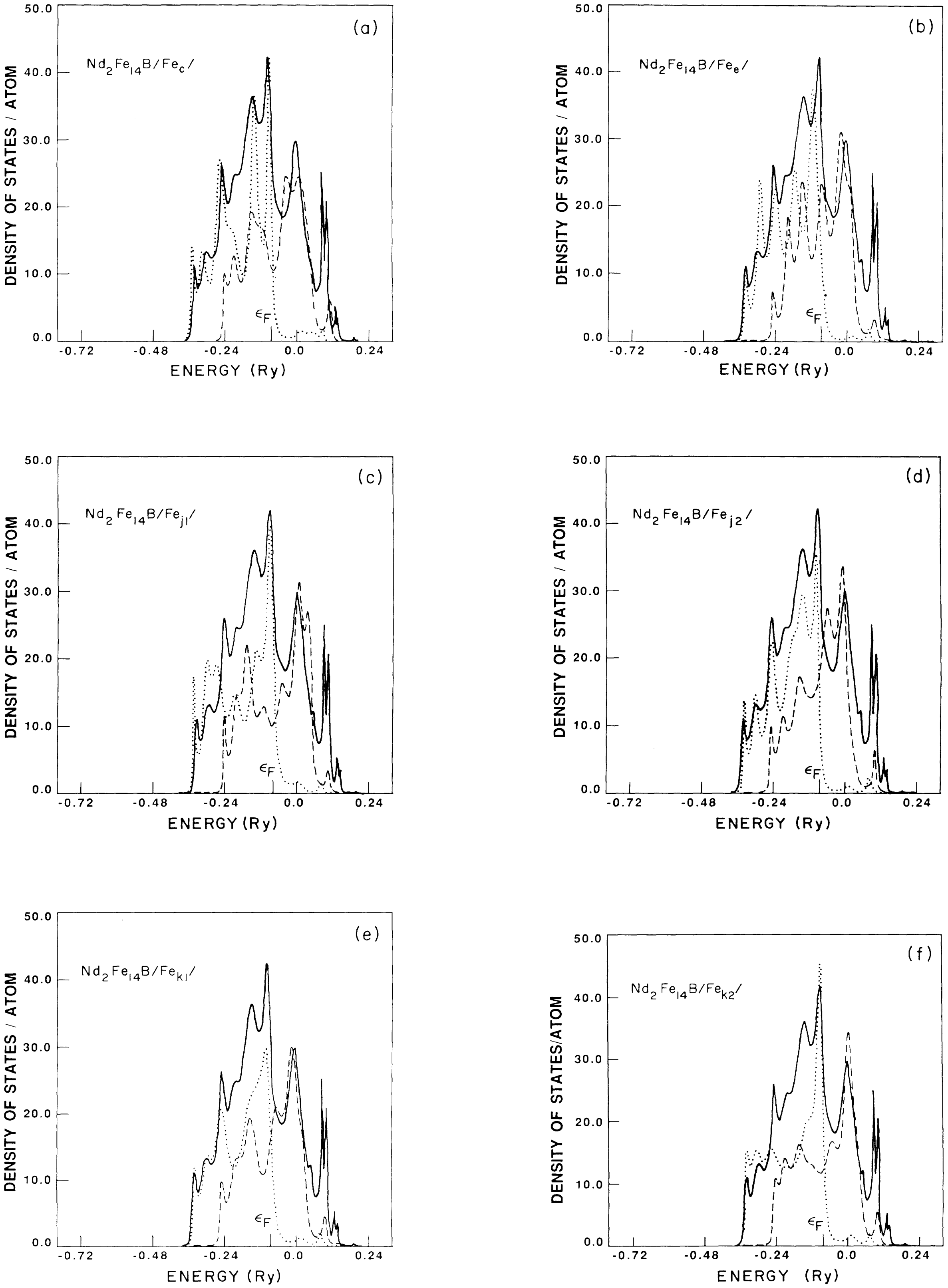

FIG. 2. The local density of states on the (a) Fe (4*c*), (b) Fe (4*e*), (c) Fe ($8j_1$), (d) Fe ($8j_2$), (e) Fe ($16k_1$), and (f) Fe ($16k_2$) sites in $Nd_2Fe_{14}B$. Solid line, total density of states; dotted line, majority-spin-up local density of states; dashed line, minority-spin-down local density of states.

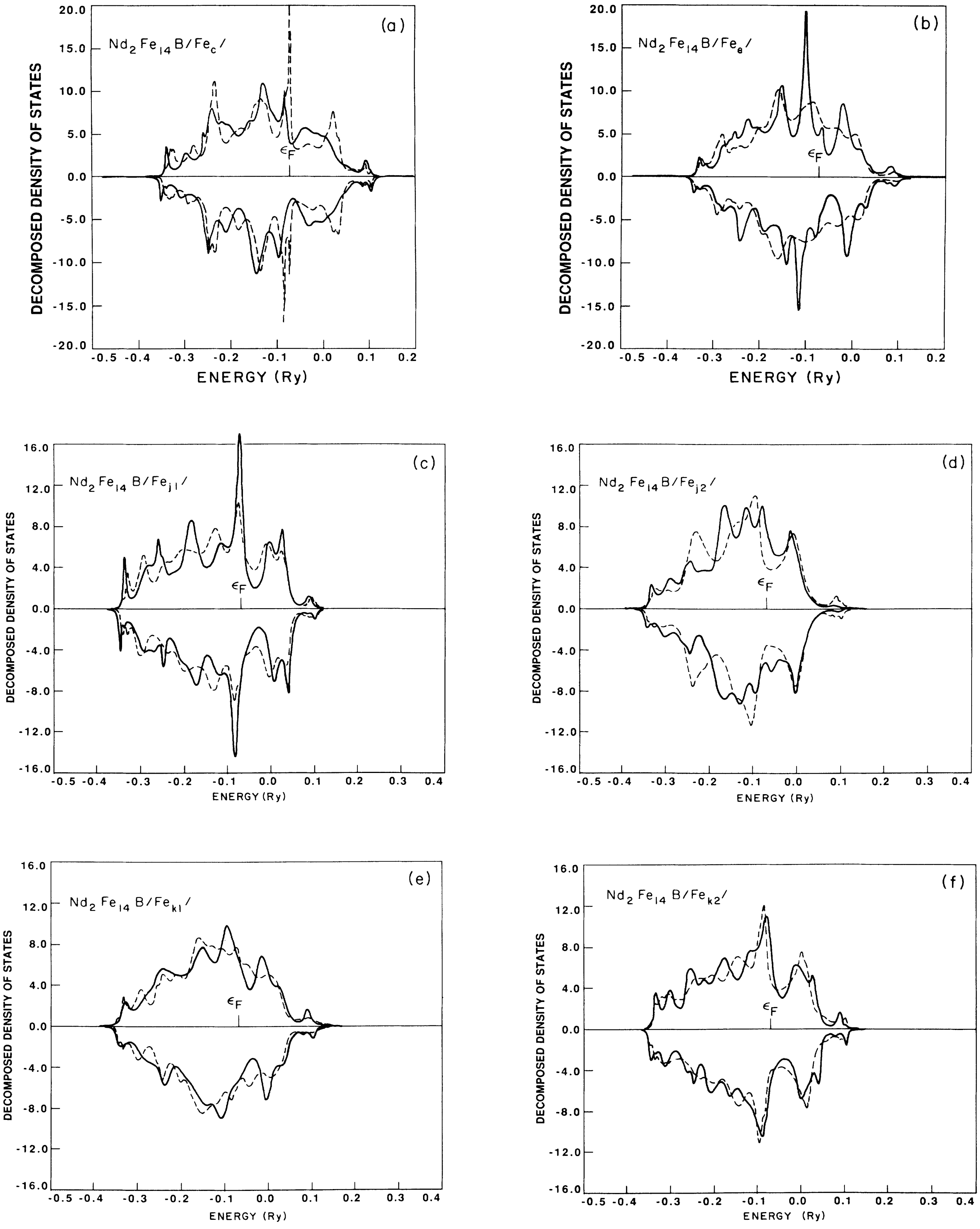

FIG. 3. The decomposed local density of states on the (a) Fe (4*c*), (b) Fe (4*e*), (c) Fe ($8j_1$), (d) Fe ($8j_2$), and (e) Fe ($16k_1$) and (f) Fe ($16k_2$) sites in $Nd_2Fe_{14}B$. The solid line corresponds to the density of states with $m_l=\pm 2$; the dashed line corresponds to the density of states with $m_l=\pm 1$.

tion of iron. The fact that pure Gd_2Fe_{17} has an easy-plane anisotropy can be explained by our calculations. A very low orbital moment was calculated on Fe(I) (6*g*) and Fe(III) (12*k*) sites (see Table IV); this suggests local easy-plane-anisotropy preference.

The average orbital moment on iron sites in $Nd_2Fe_{14}B$ is higher than in Y_2Fe_{17}; this explains why uniaxial anisotropy is observed in $Y_2Fe_{14}B$ and $Nd_2Fe_{14}B$, unlike Y_2Fe_{17}, where easy-plane anisotropy is present.

In Figs. 2–5 we present the calculated local density of states and decomposed density of states for different projections of the orbital moment on the *c* axis of $Nd_2Fe_{14}B$ and Y_2Fe_{17} compounds. The calculated local density of state is quite sensitive to the local coordination atoms. For example, j_1 and k_2 sites have the same Fe coordination number in plane and above the plane (1 and 6, respectively). Also, the coordination numbers below the plane are comparable (2 for j_1 and 3 for k_2 sites).[4] We can see the similarity in the shape of the density of states in Figs. 2(c) and 2(f). In $Nd_2Fe_{14}B$ the Fermi energy crosses the density of states on iron sites for the majority-spin electrons close to the very-high-density and minority-spin electrons at the minimum. Thus iron sites behave as strong ferromagnets. In Y_2Fe_{17} this is not true, except for 4*f* sites. As we can see from Tables III and IV, we obtain enhancement of the local moment on iron sites in $Nd_2Fe_{14}B$ and on the 4*f* site in Y_2Fe_{17}. Further analysis can be done; however, for us the most interesting result is the decomposed density of states for different *l*,*m* projections. The orbital moment is easily

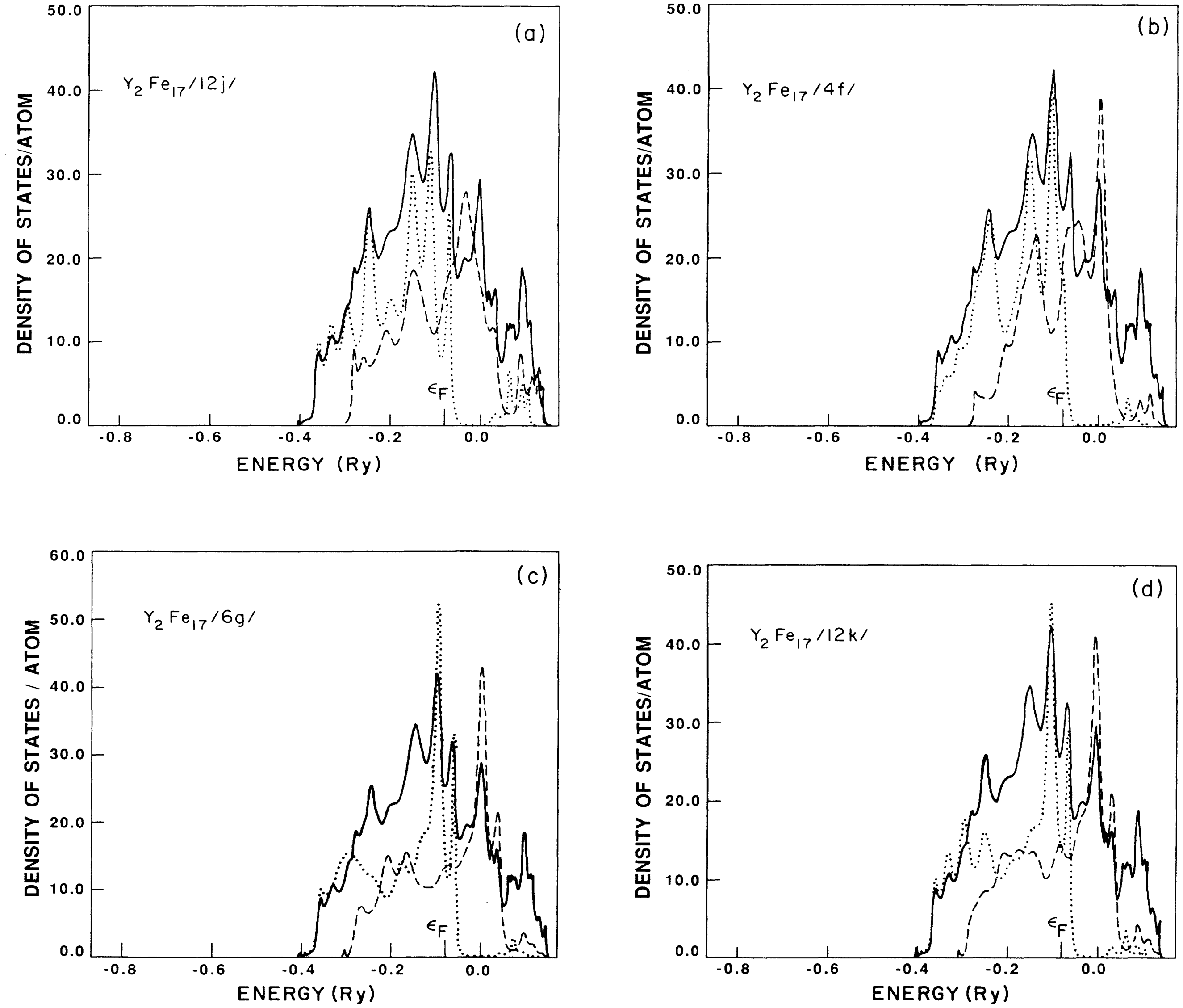

FIG. 4. The local density of states on the (a) Fe(II), (b) Fe(IV), (c) Fe(I), and (d) Fe(III) sites in Y_2Fe_{17}. Solid line, total density of states; dotted line, majority-spin-up local density of states; dashed line, minority-spin-down local density of states.

calculated from formula (11); it is the summation of the corresponding fields of the projected density of states below the Fermi energy multiplied by appropriate coefficients. From Fig. 3(d) we can see that on the j_2 site for $m = 2$ there is a high peak just below the Fermi energy and for $m = -2$ a peak just above the Fermi energy. Thus, as a result of integration up to the Fermi energy, we get a high orbital moment on the j_2 site. The d electrons are strongly localized and they contribute most to the magnetic moment; however, it would be interesting to perform similar calculations with s and p electrons included.

In conclusion, we would like to stress that the method of calculation presented here is especially useful for finding the differences between the various sites. These are not *ab initio* calculations and we have to fit few parameters, which perhaps makes our calculations not that suitable for pure materials.

ACKNOWLEDGMENTS

We would like to mention that the local-spin contribution of the moment in Y_2Fe_{17} and $Nd_2Fe_{14}B$ was calculated in the Physics Department at the University of Durham, UK. B.S. is grateful to Dr. N. Beer for receiving access to his computer program, which enabled the calculation of the paramagnetic density of states using the continued-fraction method. We are grateful to the Physics Department of Queen's University for technical assistance in the preparation of this publication and to Dr. John Rowat for comments on the manuscript. This work was supported by the National Science Foundation through Grant No. CHE-8208048.

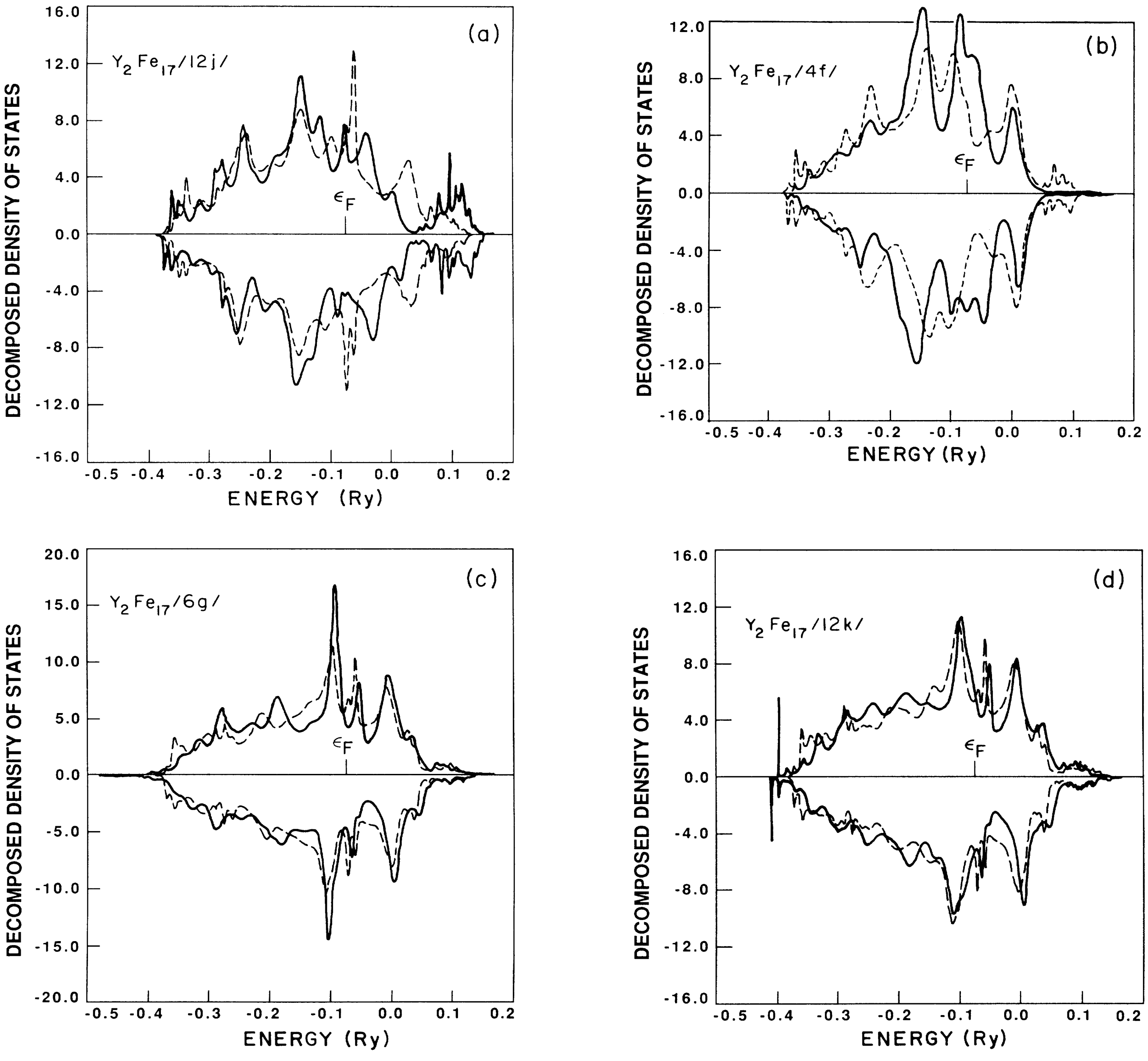

FIG. 5. The decomposed local density of states on the (a) Fe(II), (b) Fe(IV), (c) Fe(I), and (d) Fe(III) sites in Y_2Fe_{17}. The solid line corresponds to the density of states with $m_l = \pm 2$; dashed line corresponds to the density of states with $m_l = \pm 1$.

*Present address: Department of Chemistry, Queen's University, Kingston, Ontario, Canada K7L 3N6.

[1] B. Szpunar and P. A. Lindgard, J. Phys. F **9**, L55 (1979).

[2] J. F. Herbst, J. J. Croat, F. E. Pinkerton, and W. B. Telon, Phys. Rev. B **29**, 4176 (1984).

[3] G. Givord, M. S. Li, and J. M. Moreau, Solid State Commun. **50**, 497 (1984).

[4] J. F. Herbst, J. J. Croat, and W. B. Yelon, J. Appl. Phys. **57**, 4086 (1985).

[5] E. B. Boltich, E. Oswald, M. Q. Huang, S. Hirosawa, W. E. Wallace, and E. Burzo, J. Appl. Phys. **57**, 4106 (1985).

[6] B. Szpunar, Acta Phys. Polon. A **60**, 791 (1981).

[7] D. Givord and H. S. Li, J. Appl. Phys. **57**, 4 (1985); **57**, 100 (1985).

[8] R. Kamal and Y. Anderson (unpublished).

[9] E. Burzo and W. E. Wallace (unpublished).

[10] R. Grossinger, G. Hilscher, H. Kirchmayr. H. Sassik, R. Strnat, and G. Wiesinger, Physica **130B**, 307 (1985).

[11] B. Szpunar and B. Kozarzewski, Phys. Status Solidi B **82**, 205 (1977).

[12] B. Szpunar, J. Phys. F **12**, 759 (1982).

[13] B. Szpunar, Physica **130B**, 29 (1985).

[14] P. A. Lindgard and B. Szpunar, J. Magn. Magn. Mater. **7**, 124 (1978).

[15] N. C. Koon, B. N. Das, M. Rubinstein, and J. Tyson, J. Appl. Phys. **57**, 4032 (1985).

[16] P. Turchi, F. Ducastelle, and G. Treglia, J. Phys. C **15**, 2891 (1982).

[17] W. Beer and D. G. Pettifor, in *The Electronic Structure of Complex Systems,* Vol. 113 of The NATO Advanced Study Institute Series B, edited by P. Phariseau and W. M. Tennerman (Plenum, New York, 1984), p. 769.

[18] B. Szpunar and J. Szpunar, J. Appl. Phys. **57**, 4130 (1985).

[19] F. Herman and S. Skillman, *Atomic Structure Calculations* (Prentice-Hall, Englewood Cliffs, NJ, 1963).

[20] B. Szpunar, Phys. Lett. **115A**, 157 (1986).

[21] D. G. Pettifor, J. Phys. F **7**, 613 (1977).

[22] J. C. Slater and G. F. Koster, Phys. Rev. **94**, 1498 (1954).

[23] H. Shiba, Prog. Theor. Phys. **46**, 77 (1971).

[24] B. N. Cox, M. A. Coulthard, and P. Loyd, J. Phys. F **4**, 807 (1974).

[25] B. Szpunar and W. E. Wallace, Lanthanide Actinide Res. **1**, 335 (1986).

[26] R. Fruchart, Ph. L'Heritier, P. Dalmas De Reotier, D. Fruchart, P. Wolfers, J. M. D. Coey, L. P. Ferreira, R. Guillen, P. Vulliet, and A. Yaouanc, J. Phys. F (to be published).

[27] B. Szpunar and W. E. Wallace, Phys. Rev. B **35**, 1988 (1987).

[28] J. M. D. Coey and J. F. Herbst (private communication).

[29] M. Kawakami, J. Phys. F **11**, 267 (1981).